Journal of Sound and Vibration (1998) **214**(2), 245–260
Article No. sv981546

INFLUENCE OF ATTACHED LIQUID LAYERS ON FREE HYDROELASTIC VIBRATIONS OF A CYLINDRICAL SECTOR SHELL IN A ZERO-GRAVITY CONDITION

M. Chiba

Department of Mechanical Engineering, *Iwate University*, *Morioka* 020-8551, *Japan*

H. F. Bauer

Institut für Raumfahrttechnik, *Universität der Bundeswehr München*, *D*-85577 *Neubiberg*, *Germany*

AND

H. Sasaki

Japan Air Self-Defense Force, *Gifu* 504-0912, *Japan*

(*Received* 2 *April* 1997, *and in final form* 13 *January* 1998)

A theoretical analysis on the hydroelastic behavior of a circular cylindrical sector shell, attached to incompressible and frictionless liquid layers on both its sides, has been performed in a zero-gravity environment. The motion of the section shell is described by the equations of Flügge. The coupled vibration problem has been reduced to an eigenvalue problem by applying the Galerkin method and yields the coupled natural frequencies and vibration modes as eigenvalues and eigenvectors respectively. Numerical calculations were carried out to find the influence of the parameters of the structure–liquid system. Stability boundaries of vibration modes with circumferential wave number $N = 0$ and $N = 1$ of a liquid attached inside or outside a rigid cylindrical wall were also investigated.

1. INTRODUCTION

The advent of orbital space flights and orbital space stations with long time periods in a zero- or micro-gravity environment presents one, due to the required light and very flexible structures, unique problems on the interaction of liquids and elastic structures. Cylindrical configurations seem to be the basic geometry. These hydroelastic problems will influence the design of these space structures and may lead to complicated dynamic phenomena. For this reason, it is necessary to clarify the vibration characteristics of the structure–liquid systems and determine first of all the coupled frequencies of liquid and the elastic structural oscillations. A large number of studies, theoretical and experimental, have been performed previously [1–15] for liquid containing structures mainly under gravity condition. In these studies, where the interest emphasized propellant containers in missiles, space vehicle, satellites and also large capacity oil storage tanks, the hydroelastic investigations concentrated mainly on upright circular cylindrical containers. Some problems concerning hydroelasticity under micro- or zero-gravity conditions have also been treated previously [16]. In addition some work has been performed for spinning systems in zero-gravity environment [17]. Recently [18] the coupled frequencies of an elastic sector shell and

0022–460X/98/270245 + 16 $30.00/0

frictionless liquid in zero-gravity have been determined in which axial dependency has been neglected. The three-dimensional problem, i.e., the inclusion of this dependency in the x direction was treated in [19], where the interaction of the elasticity of a cylindrical sector shell and the liquid with a free surface, held in position by mere surface tension, had been investigated.

In the following investigation, the uncoupled vibration characteristics of a sector shell without liquid and the uncoupled frequencies of incompressible liquids around a rigid curved sector wall have been determined together with the coupled problem of the total elastic and sloshing system. The sector shell was modelled as a thin cylindrical shell with clamped–clamped circumferential and simply supported boundary conditions in the axial direction. Flügge's thin shell theory has been employed. The effect of the various parameters of the hydroelastic system, such as the aspect ratio, the thickness ratio, the apex angle of the shell, the density ratio, the surface tension parameter and the thickness parameter of the liquid, have been investigated. The coupled natural frequencies have been determined and the unstable vibration region of the liquid attached inside or outside a rigid wall, where some natural frequencies disappear, has been clarified.

2. BASIC EQUATIONS

An elastic cylindrical sector shell (Figure 1) at $r = R$ and the attached liquid layers of outer thickness $(b_o - R)$ and inner thickness $(R - b_i)$ are performing oscillations under the influence of the elastic structure and the free liquid surface, if disturbed. The elastic shell, of length l (x direction), exhibits an apex angle Θ and clamped boundaries in the circumferential direction. The shell is simply supported at its ends $x = 0$ and l. The liquids of density ρ_j ($j = o$ outer, i inner) and surface tensions σ_j are allowed to freely slip at the rigid sector walls $\theta = 0$, Θ. One treats here a wetting liquid system which remains in contact with the walls throughout the motion. The contact angle of the liquids with the side walls is assumed to remain $\pi/2$ or in the immediate vicinity of $\pi/2$, thus rendering an equilibrium surface of the liquid which is of circular cylindrical form. For small liquid velocities and small elastic deformations the governing equations may be linearized. With

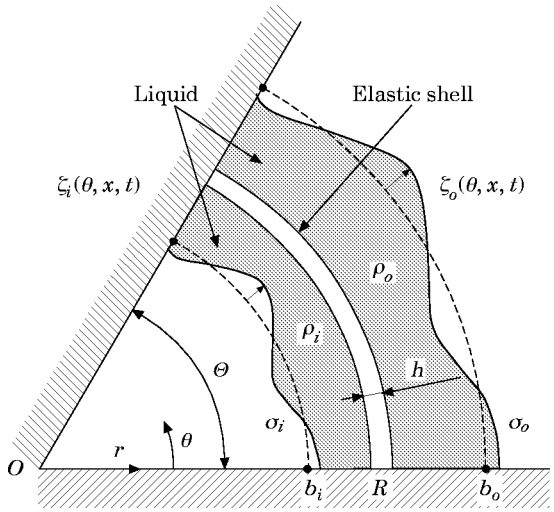

Figure 1. Elastic sector cylindrical shell with attached liquids.

the liquid motion assumed to be irrotational, the continuity equation $\operatorname{div} \vec{v} = 0$ leads to the Laplace equations for the velocity potential Φ_j.

$$\Delta\Phi_j = 0, \qquad R < r < b_o, \qquad b_i < r < R, \qquad 0 < \theta < \Theta$$
$$\Delta = (1/r)(\partial/\partial r)(r\,\partial/\partial r) + 1/r^2(\partial^2/\partial\theta^2) + \partial^2/\partial x^2, \tag{1}$$

which have to be solved with the appropriate boundary conditions. Subscript j ($= o, i$) corresponds to the outer ($j = o$) and the inner ($j = i$) liquid attached around the elastic wall respectively.

The boundary conditions at the rigid side walls are

$$(1/r)\Phi_{j,\theta} = 0, \qquad R < r < b_o, \qquad b_i < r < R, \qquad \theta = 0, \Theta, \tag{2}$$

while at the free liquid surfaces the kinematic conditions are

$$\zeta_{j,t} = \Phi_{j,r}, \qquad r = b_j, \qquad 0 < \theta < \Theta \tag{3}$$

and the dynamic conditions

$$-\rho_j\Phi_{j,t} \pm (\sigma_j/b_j^2)(\zeta_j + \zeta_{j,\theta\theta} + b_j^2\zeta_{j,xx}) = 0, \qquad r = b_j, \qquad 0 < \theta < \Theta, \tag{4}$$

where $\zeta_j = \zeta_j(\theta, x, t)$ are the free liquid surface displacement. In equation (4), $+$ and $-$ correspond to the dynamic condition of the outer and the inner liquid respectively. At the shell surface, the compatibility condition

$$W_{,t} = \Phi_{j,r}, \qquad r = R, \qquad 0 < \theta < \Theta, \tag{5}$$

has to be satisfied, so that the velocity of the shell is equal to the velocities of the liquids at the shell wall. This is valid for wetting liquid and small oscillation frequencies, where no cavity effects may be present.

With the displacements of the middle surface of the elastic sector shell in the x, θ and r directions, as U, V and W respectively, the equations of motion of the shell are given by using the equations of Flügge [20],

$$R^2U_{,xx} + \tfrac{1}{2}(1-\nu)U_{,\theta\theta} + \tfrac{1}{2}(1+\nu)RV_{,\theta x} + \nu RW_{,x} - [\rho_s(1-\nu^2)/E]R^2U_{,tt}$$
$$\underline{+\,\bar{k}\{\tfrac{1}{2}(1-\nu)U_{,\theta\theta} - R^3W_{,xxx} + \tfrac{1}{2}(1-\nu)RW_{,x\theta\theta}\}} = 0, \tag{6}$$

$$\tfrac{1}{2}(1+\nu)RU_{,\theta x} + V_{,\theta\theta} + \tfrac{1}{2}(1-\nu)R^2V_{,xx} + W_{,\theta} - [\rho_s(1-\nu^2)/E]R^2V_{,tt}$$
$$\underline{+\,(\bar{k}/2)R^2\{3(1-\nu)V_{,xx} - (3-\nu)W_{,xx\theta}\}} = 0, \tag{7}$$

$$\nu RU_{,x} + V_{,\theta} + W + (h^2R^2/12)\nabla^4W + [\rho_s(1-\nu^2)/E]R^2W_{,tt}\underline{+\,2\bar{k}W_{,\theta\theta} + \bar{k}W}$$
$$\underline{-\,R\bar{k}\{R^2U_{,xxx} - \tfrac{1}{2}(1-\nu)U_{,x\theta\theta} + (R/2)(3-\nu)V_{,xx\theta}\}} = (R^2/J)(\rho_o\Phi_{o,t} - \rho_i\Phi_{i,t}), \tag{8}$$

where $0 \leqslant x \leqslant l$, and

$$J = Eh/(1-\nu^2), \qquad \nabla^2 = \partial^2/\partial x^2 + (1/R^2)\,\partial^2/\partial\theta^2, \qquad \bar{k} = h^2/12R^2. \tag{9}$$

It may be noted that the influence of the frictionless liquids appears only on the right side of equation (8). If in the above equations the underlined terms are neglected, the basic equations of Donnell, which are widely used as shallow shell equations, are obtained. In non-dimensional form the above equations (1)–(8) yield

$$\Delta'\phi_j = 0, \qquad 1 < \rho < d_o, \qquad d_i < \rho < 1, \qquad 0 < \psi < \pi, \tag{10}$$

$$(1/\rho)\phi_{j,\psi} = 0, \qquad 1 < \rho < d_o, \qquad d_i < \rho < 1, \qquad \psi = 0, \pi, \tag{11}$$

$$\overline{\zeta}_{j,\tau} = \phi_{j,\rho}, \qquad \rho = d_j, \qquad 0 < \psi < \pi, \tag{12}$$

$$-\bar{\rho}_j d_j^2 \phi_{j,\tau} \pm \bar{\sigma}_j \beta^2 \{\overline{\zeta}_j + (1/4\alpha^2)\overline{\zeta}_{j,\psi\psi} + (d_j/\beta)^2 \overline{\zeta}_{j,\xi\xi}\} = 0, \qquad \rho = d_j, \qquad 0 < \psi < \pi, \tag{13}$$

$$-\bar{\rho}_j d_j^2 \phi_{j,\tau\tau} \pm \bar{\sigma}_j \beta^2 \{\phi_{j,\rho} + (1/4\alpha^2)\phi_{j,\rho\psi\psi} + (d_j/\beta)^2 \phi_{j,\rho\xi\xi}\} = 0, \qquad \rho = d_j, \qquad 0 < \psi < \pi, \tag{14}$$

$$w_{,\tau} = \overline{h}\phi_{j,\rho}, \qquad \rho = 1, \tag{15}$$

$$L_1 \equiv u_{,\xi\xi} + \tfrac{1}{2}(1-\nu)\hat{\beta}^2 u_{,\psi\psi} + \tfrac{1}{2}(1+\nu)\hat{\beta} v_{,\psi\xi} + \nu w_{,\xi} - u_{,\tau\tau} + \underline{\overline{k}\{\tfrac{1}{2}(1-\nu)\hat{\beta}^2 u_{,\psi\psi} - (1/\beta^2) w_{,\xi\xi\xi} + (1/8\alpha^2)(1-\nu) w_{,\xi\psi\psi}\}} = 0, \tag{16}$$

$$L_2 \equiv \tfrac{1}{2}(1+\nu)\hat{\beta} u_{,\psi\xi} + \hat{\beta}^2 v_{,\psi\psi} + \tfrac{1}{2}(1-\nu) v_{,\xi\xi} + \hat{\beta} w_{,\psi} - v_{,\tau\tau} + \underline{(\overline{k}/2)\{3(1-\nu)v_{,\xi\xi} - (1/2\alpha\beta)(3-\nu) w_{,\xi\xi\psi}\}} = 0, \tag{17}$$

$$L_3 \equiv \nu u_{,\xi} + \hat{\beta} v_{,\psi} + w + (\overline{k}/\beta^4)\overline{\nabla}^4 w + (1/\beta^2) w_{,\tau\tau} + \underline{\overline{k}\{(1/2\alpha^2) w_{,\psi\psi} + w - (1/\beta^2) u_{,\xi\xi\xi} + (1/8\alpha^2)(1-\nu) u_{,\xi\psi\psi} - (1/4\alpha\beta)(3-\nu) v_{,\xi\xi\psi}\}} = (1/\beta^2)(\bar{\rho}_o \phi_{o,\tau} - \bar{\rho}_i \phi_{i,\tau}) \tag{18}$$

where the dimensionless values

$$\xi = (\pi/l)x, \qquad \psi = \theta/2\alpha, \qquad \tau = \Omega_0 t, \qquad \beta = l/R\pi, \qquad \hat{\beta} = \beta/2\alpha,$$

$$\Omega_0 = (\pi/l)\sqrt{E/\rho_s(1-\nu^2)}, \qquad (u, v) = (R\pi/lh)(U, V), \qquad w = W/h,$$

$$\bar{\sigma}_j = \sigma_j(1-\nu^2)/RE, \qquad \omega = \Omega/\Omega_0, \qquad \rho = r/R, \qquad \overline{\zeta}_j = (R/h^2)\zeta_j, \qquad \overline{h} = R/h,$$

$$\overline{k} = 1/12\overline{h}^2, \qquad d_j = b_j/R, \qquad \bar{\rho}_j = \rho_j/\rho_s, \qquad \Theta = 2\pi\alpha, \qquad 0 < \alpha < 1,$$

$$\phi_j = \Phi_j/\Omega_0 h^2, \qquad \overline{\nabla}^2 = \partial^2/\partial\xi^2 + \hat{\beta}^2\, \partial^2/\partial\psi^2,$$

$$\Delta' = \partial^2/\partial\rho^2 + (1/\rho)\,\partial/\partial\rho + (1/4\alpha^2\rho^2)\,\partial^2/\partial\psi^2 + (1/\beta^2)\,\partial^2/\partial\xi^2 \tag{19}$$

have been used. Equation (14) is the combined free surface condition, as obtained from equations (3) and (4) or (12) and (13). In equations (13) and (14), the + and − correspond to the equation when the liquid is attached to the outer and inner surface of the shell respectively. The values ρ_s, ρ_j are the density of the shell and liquids respectively, E, ν are Young's modulus of elasticity and Poisson's ratio of the shell, t and Ω are time and natural circular frequency respectively. l could either be considered as the length of the shell in the axial direction or the length of one half of the axial mode. ω, d_j and $\overline{h}$ are the non-dimensional parameters concerned with the natural frequency, liquid thicknesses and shell thickness respectively.

3. METHOD OF SOLUTION

The solution of the Laplace equation (10) by separation of variables satisfying the rigid wall boundary condition (11) renders the equations

$$\phi_o(\xi, \varphi, \rho, \tau) = \mathrm{i}\omega\, \mathrm{e}^{\mathrm{i}\omega\tau} \sum_m \sum_k \left\{ A_{km} I_{k/2\alpha}\left(\frac{m}{\beta}\rho\right) + B_{km} K_{k/2\alpha}\left(\frac{m}{\beta}\rho\right)\right\} \sin m\xi \cos k\psi,$$

$$m = 1, 2, \ldots, \qquad k = 0, 1, 2, \ldots \tag{20}$$

$$\phi_i(\xi, \varphi, \rho, \tau) = \mathrm{i}\omega\, \mathrm{e}^{\mathrm{i}\omega\tau} \sum_m \sum_k \left\{ C_{km} I_{k/2\alpha}\left(\frac{m}{\beta}\rho\right) + D_{km} K_{k/2\alpha}\left(\frac{m}{\beta}\rho\right)\right\} \sin m\xi \cos k\psi,$$

$$m = 1, 2, \ldots, \qquad k = 0, 1, 2, \ldots, \tag{21}$$

where A_{km}, B_{km}, C_{km} and D_{km} are unknown constants, and $\mathrm{I}_{k/2\alpha}$ and $\mathrm{K}_{k/2\alpha}$ are modified Bessel functions of order $k/2\alpha$ and of the first and second kind.

3.1. UNCOUPLED LIQUID MOTION WITH FREELY SLIPPING EDGES

For a rigid sector wall the boundary condition is

$$\partial\phi_j/\partial\rho = 0 \quad \text{at} \quad \rho = d_j, \qquad 0 < \psi < \pi, \tag{22}$$

which yields together with the combined free surface condition (14) the uncoupled frequencies of the liquid as

$$\begin{aligned}\Omega_{km}^2 = {} & (\sigma_j/\rho_j R^3)(md_j/\beta)[(md_j/\beta)^2 + (k/2\alpha)^2 - 1] \\ & \times \{\mathrm{I}'_{k/2\alpha}(m/\beta)\mathrm{K}'_{k/2\alpha}([m/\beta]d_j) - \mathrm{I}'_{k/2\alpha}([m/\beta]d_j)\mathrm{K}'_{k/2\alpha}(m/\beta)\} \\ & \times \{\mathrm{I}'_{k/2\alpha}(m/\beta)\mathrm{K}_{k/2\alpha}([m/\beta]d_j) - \mathrm{I}_{k/2\alpha}([m/\beta]d_j)\mathrm{K}'_{k/2\alpha}(m/\beta)\}\end{aligned} \tag{23}$$

The prime $'$ is the derivative with respect to the argument.

3.2. COUPLED MOTION

The coupled structure–liquid system is obtained from equations (14), (16–18) by observing the compatibility condition (15). Assuming $w = \mathrm{e}^{\mathrm{i}\omega\tau} \Sigma_m \Sigma_n G_{nm} \Psi_n(\psi) \sin m\xi$ (see equation (33)) and multiplying it by $\cos k\psi\, \mathrm{d}\psi$ and integrating and by observing the orthogonality condition, one obtains from the compatibility conditions (15) the expressions

$$B_{km} = \left\{\frac{2}{\overline{h}\pi(\delta_{k0}+1)} \sum_n G_{nm}\kappa_{nk} - A_{km}\mathrm{I}'_{k/2\alpha}\left(\frac{m}{\beta}\right)\right\}\left[1/K'_{k/2\alpha}\left(\frac{m}{\beta}\right)\right], \qquad k = 0, 1, 2, \ldots, \tag{24}$$

$$D_{km} = \left\{\frac{2}{\overline{h}\pi(\delta_{k0}+1)} \sum_n G_{nm}\kappa_{nk} - C_{km}\mathrm{I}'_{k/2\alpha}\left(\frac{m}{\beta}\right)\right\}\left[1/K'_{k/2\alpha}\left(\frac{m}{\beta}\right)\right], \qquad k = 0, 1, 2, \ldots, \tag{25}$$

where

$$\kappa_{nk} = \int_0^\pi \Psi_n(\psi) \cos k\psi\, \mathrm{d}\psi, \qquad k = 0, 1, 2, \ldots. \tag{26}$$

The free liquid surface equation (14) is combined with equations (20), (21). After eliminating B_{km}, D_{km}, with equations (24) and (25), a coupled system of k equations for A_{km}, G_{nm}, and C_{km} is obtained as

$$[(M_{1okk} \quad M_{2okn}) - \omega^2(M_{3okk} \quad M_{4okn})]\begin{Bmatrix} A_{km} \\ G_{nm}\end{Bmatrix} = \{\mathbf{0}\}, \tag{27}$$

$$[(M_{1ikk} \quad M_{2ikn}) - \omega^2(M_{3ikk} \quad M_{4ikn})]\begin{Bmatrix} C_{km} \\ G_{nm}\end{Bmatrix} = \{\mathbf{0}\}, \tag{28}$$

where

$$M_{1jkk} = \bar{\sigma}_j \beta^2 X_{jk} \left[\mathrm{I}'_{k/2\alpha}\left(\frac{m}{\beta} d_j\right) - \mathrm{I}'_{k/2\alpha}\left(\frac{m}{\beta}\right) \mathrm{K}'_{k/2\alpha}\left(\frac{m}{\beta} d_j\right) \Big/ \mathrm{K}'_{k/2\alpha}\left(\frac{m}{\beta}\right) \right],$$

$$M_{2okn} = [2\bar{\sigma}_o \beta^2 X_{ok} / \bar{h}\pi(\delta_{k0} + 1)] \left[\mathrm{K}'_{k/2\alpha}\left(\frac{m}{\beta} d_o\right) \Big/ \mathrm{K}'_{k/2\alpha}\left(\frac{m}{\beta}\right) \right] \kappa_{nk},$$

$$M_{2ikn} = [2\bar{\sigma}_i \beta^2 X_{ik} / \bar{h}\pi(\delta_{k0} + 1)] \left[K'_{k/2\alpha}\left(\frac{m}{\beta} d_i\right) \Big/ \mathrm{K}'_{k/2\alpha}\left(\frac{m}{\beta}\right) \right] \kappa_{nk},$$

$$M_{3jkk} = \pm \bar{\rho} d_j^2 \left[\mathrm{I}'_{k/2\alpha}\left(\frac{m}{\beta}\right) \mathrm{K}_{k/2\alpha}\left(\frac{m}{\beta} d_j\right) \Big/ \mathrm{K}'_{k/2\alpha}\left(\frac{m}{\beta}\right) - \mathrm{I}_{k/2\alpha}([m/\beta] d_j) \right],$$

$$M_{4jkn} = \mp [2\bar{\rho} d_j^2 / \bar{h}\pi(\delta_{k0} + 1)] \left[\mathrm{K}_{k/2\alpha}\left(\frac{m}{\beta} d_j\right) \Big/ \mathrm{K}'_{k/2\alpha}\left(\frac{m}{\beta}\right) \right] \kappa_{nk}, \tag{29}$$

$$X_{jk} = 1 - (k/2\alpha)^2 - (d_j m/\beta)^2. \tag{30}$$

Next, one considers the equation of motion of the sector shell assuming that the straight edge along $\psi = 0, \pi$ is clamped, and that the curved edges $\xi = 0, \pi$ are simply supported. Therefore the boundary conditions of the shell are

$$u = v = w = w_{,\psi} = 0 \quad \text{at } \psi = 0, \pi, \tag{31}$$

and

$$n_x = v = w = m_x = 0 \quad \text{at } \xi = 0, \pi, \tag{32}$$

where

$$n_x = u_{,\xi} + \nu\{(\beta/2\alpha) v_{,\psi} + w\} - (\bar{k}/\beta^2) w_{,\xi\xi},$$

$$m_x = w_{,\xi\xi} + \nu\{(\beta^3/2\alpha) v_{,\psi} + (\beta/2\alpha)^2 w_{,\psi\psi}\} + \beta^2 u_{,\xi}.$$

With these boundary conditions the shell displacements u, v and w may be represented in the form

$$\begin{Bmatrix} u(\xi, \psi, \tau) \\ v(\xi, \psi, \tau) \\ w(\xi, \psi, \tau) \end{Bmatrix} = \mathrm{e}^{\mathrm{i}\omega\tau} \sum_m \sum_n \begin{Bmatrix} F_{nm} \Psi_n(\psi) \\ F_{nm} \Psi_n(\psi) \\ G_{nm} \Psi_n(\psi) \end{Bmatrix} \begin{Bmatrix} \cos m\xi \\ \sin m\xi \\ \sin m\xi \end{Bmatrix}, \qquad n, m = 1, 2, \ldots, \tag{33}$$

where E_{nm}, F_{nm}, G_{nm} are unknown constants. $\Psi_n(\psi)$ is a beam function which satisfies the clamped–clamped boundary conditions.

$$\Psi_n(\psi) = \Psi_{n,\psi}(\psi) = 0 \quad \text{at } \psi = 0, \pi. \tag{34}$$

Introducing equation (33) into equations (16–18), and applying the Galerkin method, one obtains

$$\int_0^{\pi}\int_0^{\pi}\begin{pmatrix}L_1(\xi,\psi)\\L_2(\xi,\psi)\\L_3(\xi,\psi)\end{pmatrix}\Psi_p(\psi)\begin{pmatrix}\cos q\xi\\ \sin q\xi\\ \sin q\xi\end{pmatrix}\mathrm{d}\psi\ \mathrm{d}\xi = 0, \qquad p = 1, 2, \ldots, \qquad q = 1, 2, \ldots, \tag{35}$$

Rearranging the results in a matrix form yields finally

$$\left[\begin{pmatrix}0&0&0&0&M_{5pn}&M_{6pn}&M_{7pn}\\0&0&0&0&M_{6pn}&M_{8pn}&M_{9pn}\\0&0&0&0&M_{7pn}&M_{9pn}&M_{10pn}\end{pmatrix} - \omega^2\begin{pmatrix}0&0&0&0&\delta_{pn}&0&0\\0&0&0&0&0&-\delta_{pn}&0\\M_{11opk}&M_{12opk}&M_{11ipk}&M_{12ipk}&0&0&\delta_{pn}/\beta^2\end{pmatrix}\right]$$

$$\times\begin{Bmatrix}A_{km}\\B_{km}\\C_{km}\\D_{km}\\E_{nm}\\F_{nm}\\G_{nm}\end{Bmatrix} = \{\mathbf{0}\}, \tag{36}$$

where

$$M_{5pn} = m^2\delta_{pn} - \tfrac{1}{2}(1-\nu)\hat{\beta}^2\mathrm{J}_{pn}^{02} \underline{- \tfrac{1}{2}\overline{k}(1-\nu)\hat{\beta}^2\mathrm{J}_{pn}^{02}},$$

$$M_{6pn} = (\hat{\beta}/2)m(1+\nu)\mathrm{J}_{pn}^{01},$$

$$M_{7pn} = m\nu\delta_{pn}\underline{+ (m^3/\beta^2)\overline{k}\delta_{pn} + (m/8\alpha^2)\overline{k}(1-\nu)\mathrm{J}_{pn}^{02}},$$

$$M_{8pn} = \hat{\beta}^2\mathrm{J}_{pn}^{02} - (m^2/2)(1-\nu)\,\delta_{pn}\underline{- (3m^2/2)\overline{k}(1-\nu)\delta_{pn}}.$$

$$M_{9pn} = \hat{\beta}\mathrm{J}_{pn}^{01}\underline{+ (m^2/4\alpha\beta)\overline{k}(3-\nu)\mathrm{J}_{pn}^{01}},$$

$$M_{10pn} = \delta_{np} + (\overline{k}/\beta^4)\{(m^4 + \alpha_n^4\hat{\beta}^4)\delta_{pn} - 2m^2\hat{\beta}^2\mathrm{J}_{pn}^{02}\}\underline{+ (k/2\alpha^2)\mathrm{J}_{pn}^{02} + \overline{k}\delta_{np}}$$

$$M_{11opk} = -(\bar{\rho}_o/\beta^2)\mathrm{I}_{k/2\alpha}(m/\beta)\kappa_{pk}, \qquad M_{12opk} = -(\bar{\rho}_o/\beta^2)\mathrm{K}_{k/2\alpha}(m/\beta)\kappa_{pk},$$

$$M_{11ipk} = (\bar{\rho}_i/\beta^2)\mathrm{I}_{k/2\alpha}(m/\beta)\kappa_{pk}, \qquad M_{12ipk} = \bar{\rho}_i/\beta^2\,\mathrm{K}_{k/2\alpha}(m/\beta)\kappa_{pk}, \tag{37}$$

and where

$$\mathrm{J}_{pn}^{00} = \int_0^{\pi}\Psi_p(\psi)\Psi_n(\psi)\,\mathrm{d}\psi = \delta_{pn}$$

$$\mathrm{J}_{pn}^{02} = \int_0^{\pi}\Psi_p(\psi)\Psi_n''(\psi)\,\mathrm{d}\psi = [\Psi_p\Psi_n']_0^{\pi} - \int_0^{\pi}\Psi_p'(\psi)\Psi_n'(\psi)\,\mathrm{d}\psi = -\mathrm{J}_{pn}^{11}$$

$$\mathrm{J}^{01}_{pn} = \int_0^{\pi} \Psi_p(\psi)\Psi'_n(\psi)\,\mathrm{d}\psi, \qquad \mathrm{J}^{11}_{pn} = \int_0^{\pi} \Psi'_p(\psi)\Psi'_n(\psi)\,\mathrm{d}\psi.$$

δ_{pn} is Kronecker's delta. Neglecting the influence of the liquid ($M_{11jpk} = M_{12jpk} = 0$), equation (29) reduces to the uncoupled frequency equation of the shell wall.

Combining equations (27), (28) and equation (36), one obtains

$$\left[\begin{pmatrix} M_{1okk} & 0 & 0 & 0 & M_{2okn} \\ 0 & M_{1ikk} & 0 & 0 & M_{2ikn} \\ 0 & 0 & M_{5pn} & M_{6pn} & M_{7pn} \\ 0 & 0 & M_{6pn} & M_{8pn} & M_{9pn} \\ 0 & 0 & M_{7pn} & M_{9pn} & M_{10pn} \end{pmatrix} - \omega^2 \begin{pmatrix} M_{3okk} & 0 & 0 & 0 & M_{4okn} \\ 0 & M_{3ikk} & 0 & 0 & M_{4ikn} \\ 0 & 0 & \delta_{pn} & 0 & 0 \\ 0 & 0 & 0 & -\delta_{pn} & 0 \\ M_{13pk} & M'_{13pk} & 0 & 0 & M_{14pn} \end{pmatrix} \right] \begin{Bmatrix} A_{km} \\ C_{km} \\ E_{nm} \\ F_{nm} \\ G_{nm} \end{Bmatrix} = \{\mathbf{0}\} \tag{38}$$

where

$$\begin{aligned} M_{13pk} &= -(\bar{\rho}_o/\beta^2)\kappa_{pk}[I_{k/2\alpha}(m/\beta) - \mathrm{I}'_{k/2\alpha}(m/\beta)\mathrm{K}_{k/2\alpha}(m/\beta)/\mathrm{K}'_{k/2\alpha}(m/\beta)], \\ M'_{13pk} &= (\bar{\rho}_i/\beta^2)\kappa_{pk}[\mathrm{I}_{k/2\alpha}(m/\beta) - \mathrm{I}'_{k/2\alpha}(m/\beta)\mathrm{K}_{k/2\alpha}(m/\beta)/\mathrm{K}'_{k/2\alpha}(m/\beta)], \end{aligned} \tag{39}$$

$$M_{14in} = \frac{\delta_{pn}}{\beta^2} - \frac{2\bar{\rho}_o}{\beta^2\bar{h}\pi} \sum_k \frac{1}{(\delta_{k0}+1)} \frac{\mathrm{K}_{k/2\alpha}(m/\beta)}{\mathrm{K}'_{k/2\alpha}(m/\beta)} \kappa_{nk}\kappa_{pk} + \frac{2\bar{\rho}_i}{\beta^2\bar{h}\pi} \sum_k \frac{1}{(\delta_{k0}+1)} \frac{\mathrm{K}_{k/2\alpha}(m/\beta)}{\mathrm{K}'_{k/2\alpha}(m/\beta)} \kappa_{nk}\kappa_{pk} \tag{40}$$

These are $(k + 3n)$, $k = 0, 1, \ldots, n = 1, 2, \ldots$, coupled linear algebraic equations for the unknowns A_{km}, C_{km}, E_{nm}, F_{nm}, and G_{nm}. From this one obtains the coupled natural frequencies and mode shapes of the vibration of the coupled liquid-structure system as an eigenvalue and eigenvector, respectively.

4. NUMERICAL RESULTS

The above obtained analytical results have been evaluated numerically for some special cases. Since the precision of the uncoupled vibration of a sector shell without liquid has already been shown in [19], the present paper will first present the uncoupled frequencies of a liquid attached to a rigid sector shell.

4.1. LIQUID AROUND RIGID SHELL

The uncoupled natural frequency of the liquid has been obtained by evaluating equations (27) and (28) where G_{nm} (i.e., the elastic displacement of the sector shell) has been neglected. The uncoupled natural frequency variation of the liquid attached inside the shell wall with the apex angle is presented in Figure 2(a) for $\beta = 0{\cdot}5$, $m = 1$, $\bar{\sigma}_i = 1{\cdot}0 \times 10^{-14}$ and $d_i = 1/1{\cdot}2$, $1/1{\cdot}8$. In the figure, the thick lines represent the uncoupled natural frequencies for $d_i = 1/1{\cdot}2$, while the thin lines are those for $d_i = 1/1{\cdot}8$. One notices that with increasing apex angle, α, the natural frequency of the liquid decreases. At $\alpha = 0{\cdot}5$ one can

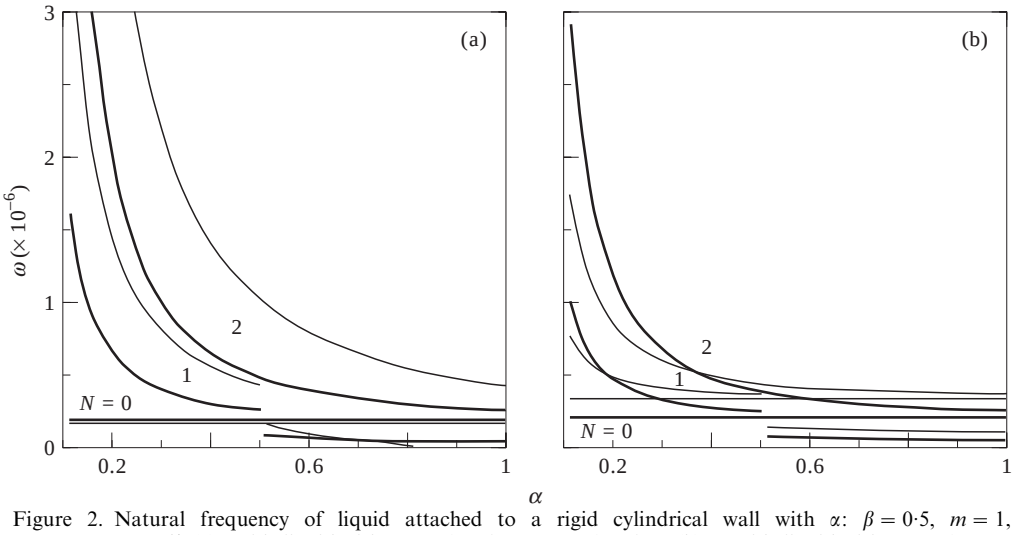

Figure 2. Natural frequency of liquid attached to a rigid cylindrical wall with α: $\beta = 0{\cdot}5$, $m = 1$, $\bar{\sigma}_i = \bar{\sigma}_o = 1{\cdot}0 \times 10^{-14}$; (a) Inside liquid with ——, $d_i = 1/1{\cdot}2$; ——, $d_i = 1/1{\cdot}8$; (b) Outside liquid with ——, $d_o = 1{\cdot}2$; ——, $d_o = 1{\cdot}8$.

see sudden drops of the natural frequency in the $N = 1$ mode for both $d_i = 1/1{\cdot}2$ and $1/1{\cdot}8$. Simultaneously, the mode $N = 1$ corresponds to the minimum natural frequency. With further increase in α, this frequency decreases to zero when $d_i = 1/1{\cdot}2$, which corresponds to an instability of the $N = 1$ mode, and there exists no stable solution for further higher value of α. The critical point at which ω is equal to zero shifts to the regions with large value of α as d_i becomes small. This means that with the inner liquid becoming thicker, for example $d_i = b_i/R = 1/1{\cdot}8$, that mode is stable for a wider range of α.

Similar tendencies have been obtained for the liquid attached outside the shell wall [19], as shown in Figure 2(b), where liquid thickness ratio $d_o = 1{\cdot}2$ and $1{\cdot}8$.

4.2. COUPLED VIBRATION WITH SECTOR SHELL AND LIQUIDS

Next, the coupled natural frequency of the elastic shell and liquids inside and outside the shell wall are considered, by investigating the effect of the liquid thickness parameters, $d_o = b_o/R$, $d_i = b_i/R$, the surface tension parameter, $\bar{\sigma}$, and the density ratio, $\bar{\rho}$ of liquid and shell density.

4.2.1. *Effect of liquid thickness*

Since this is a coupled dynamic system involving an elastic sector shell and liquids, coupled natural frequencies of both the bulging (flexural)- and sloshing-type will be obtained, in which the shell motion and the liquid surface motions are predominant respectively. As an example, the variations of coupled natural frequencies with inner liquid thickness $d_i - 1$, when $\alpha = 0{\cdot}5$, $\beta = 0{\cdot}5$, $m = 1$, $\bar{\rho} = 0{\cdot}13$, $\bar{\sigma}_i = 1{\cdot}0 \times 10^{-14}$, $\bar{h} = 50$, $d_o - 1 = 0$, i.e., without outer liquid, are shown in Figure 3. In the figure, the lowest three natural frequencies for each type are presented. In the abscissa, $d_i - 1 = 0$ and -1 correspond to the zero thickness case and fully filled case respectively. Since the magnitudes of each bulging- and sloshing-type natural frequency are far apart, different ordinates have been taken. From the figure, one can see the variation of the coupled natural frequencies with inner liquid thickness, i.e., with the increase of the liquid thickness, sloshing natural frequencies with $N = 1$ and 2 gradually increase, while the

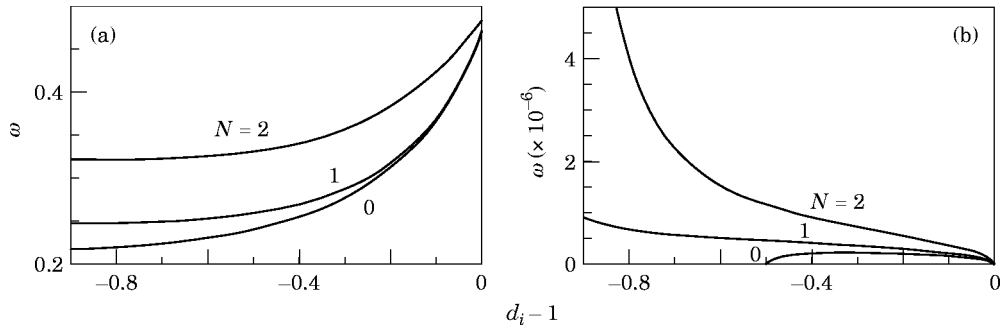

Figure 3. Effect of inner liquid thickness d_i on the coupled natural frequency: $\alpha = 0{\cdot}5$, $\beta = 0{\cdot}5$, $m = 1$, $\bar{\rho}_i = 0{\cdot}13$, $\bar{\sigma}_i = 1{\cdot}0 \times 10^{-14}$, $\bar{h} = 50$, $d_o - 1 = 0$; (a) bulging type (b) sloshing type.

bulging-type natural frequencies decrease with decrease of $d_i - 1$, which is usually due to the added mass effect of the liquid.

It should be noted here that the variation of the sloshing mode with $N = 0$ exhibits a quite different behavior than the other sloshing modes $N = 1, 2$. One observes that with an increase in liquid thickness, the natural frequency increases and then decreases, and finally reaches zero at $d_i - 1 = -0{\cdot}5$. For further increase in the inner liquid thickness, this mode disappears and becomes unstable.

The results for a decrease of the aspect ratio parameter of the shell β to 0·25 are shown in Figure 4(a). Corresponding results when the liquid is outside the shell wall [19] may be seen in Figure 4(b). Compared with the results when $\beta = 0{\cdot}5$ (shown in Figure 3), the bulging-type natural frequencies decrease in magnitude, while those of the sloshing-type exhibit a slight decrease. A significant change is that the critical value for the sloshing mode with $N = 0$ shifts from $-0{\cdot}5$ to $d_i - 1 = -0{\cdot}75$. Comparing the results in Figure 4(a) and

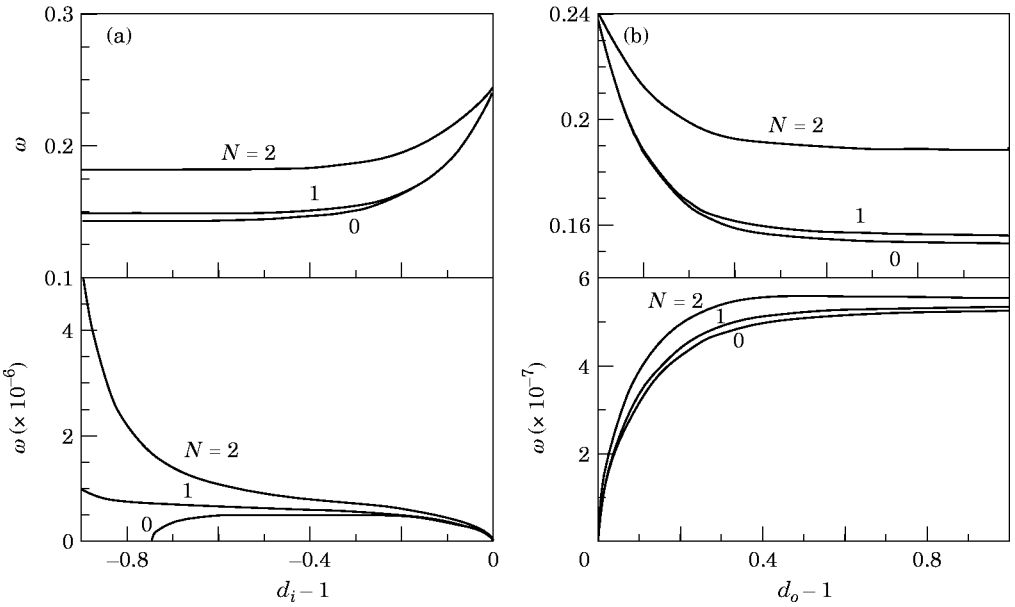

Figure 4. Effect of liquid thickness d_l on the coupled natural frequency: $\alpha = 0{\cdot}5$, $\beta = 0{\cdot}25$, $m = 1$, $\bar{\rho}_i = \bar{\rho}_o = 0{\cdot}13$, $\bar{\sigma}_i = \bar{\sigma}_o = 1{\cdot}0 \times 10^{-14}$, $\bar{h} = 50$; (a) Inner liquid with $d_o - 1 = 0$; (b) Outer liquid with $d_i - 1 = 0$. Upper graphs, bulging type; lower graphs, sloshing type.

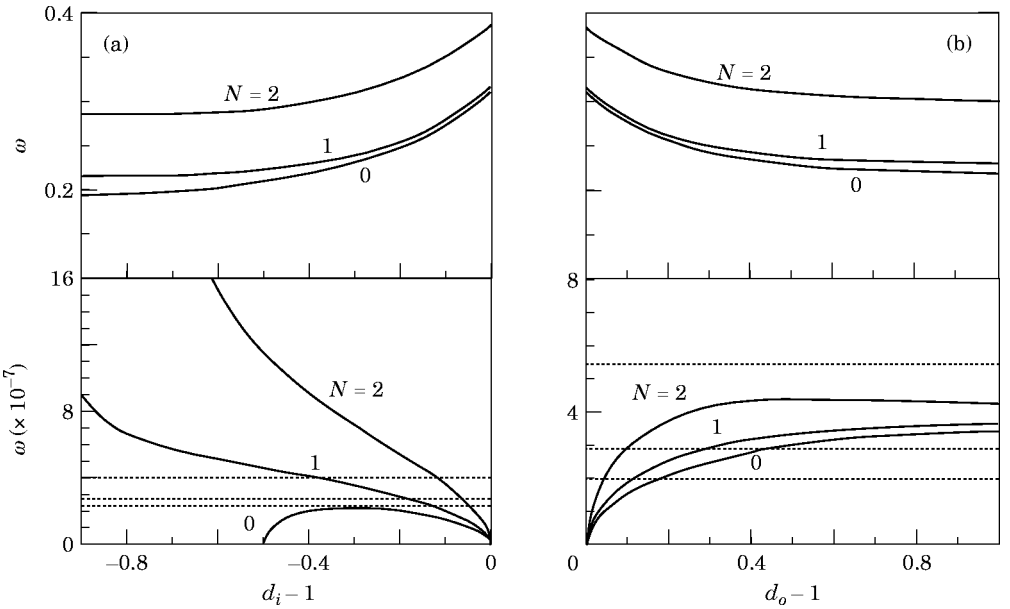

Figure 5. Effect of liquid thickness d_j on the coupled natural frequency: $\alpha = 0{\cdot}5$, $\beta = 0{\cdot}5$, $m = 1$, $\bar{\rho}_i = 0{\cdot}13$, $\bar{\sigma}_j = 1{\cdot}0 \times 10^{-14}$, $\overline{h} = 50$; (a) Inner liquid with $d_o - 1 = 0{\cdot}25$; (b) Outer liquid with $d_i - 1 = -0{\cdot}2$. Upper graphs, bulging type; lower graphs, sloshing type.

4(b), i.e., for liquid in the shell to that out of the shell, one observes that the tendency of the frequency variation for the bulging-type is similar, but that for the sloshing-type is quite different. With the decrease in thickness of the layer the sloshing frequency decreases for the inside liquid and increases for the liquid layer outside the shell.

In the above results so far, only the case when the liquid is attached to one side of the shell is presented. Hereafter, the case when the liquids are attached to both sides of the shell wall will be considered. Such a case is shown in Figures 5(a) and 5(b). In Figure 5(a), the natural frequency variations with inner liquid are shown when the outer liquid is $d_o - 1 = 0{\cdot}25$, which corresponds to the system of Figure 3 with no liquid on the outside, i.e., $d_o = 1$, while in Figure 5(b) those with the outer liquid are shown when the inner liquid $d_i - 1 = -0{\cdot}2$.

In Figures 5(a) and 5(b), dashed lines correspond to the results for sloshing natural frequency of the outer and the inner liquid respectively. A comparison of the results in Figure 5(a) and Figure 3 shows that the bulging-type natural frequency decreases due to the existence of the mass of the outer liquid in magnitude, while that of the sloshing-type does not exhibit much change. The ordinates are modified to show the results in a more lucid form. Similar results for the sector shell of very thin thickness with $\overline{h} = 1000$ are shown in Figures 6(a) and 6(b). When the results of Figure 5 when $\overline{h} = 50$ are compared with those of Figure 6, the bulging-type natural frequencies, due to the increased flexibility of the shell, significantly decrease, while those of the sloshing liquids do not show much change.

4.2.2. *Effect of surface tension parameter* $\bar{\sigma}$

In the results so far, the values of the tension parameters, $\bar{\sigma}_i$ and $\bar{\sigma}_o$, were taken as $1{\cdot}0 \times 10^{-14}$. From the definition of this parameter, $\bar{\sigma}_j = \sigma_j(1 - \nu^2)/(RE)$; $j = i$ and o, j, is the ratio of the surface tension of liquids and the stiffness of a shell in terms of Young's modulus E. A small value of $\bar{\sigma}_j$ means that the surface tension is smaller than the shell's

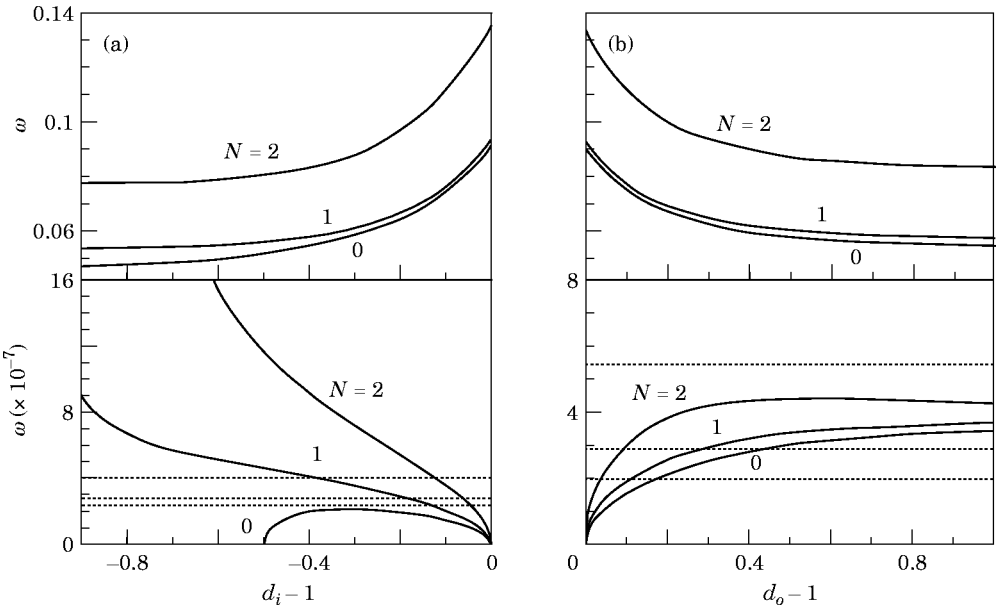

Figure 6. Effect of liquid thickness d_j on the coupled natural frequency: $\alpha = 0{\cdot}5$, $\beta = 0{\cdot}5$, $m = 1$, $\bar{\rho}_j = 0{\cdot}13$, $\bar{\sigma}_j = 1{\cdot}0 \times 10^{-14}$, $\overline{h} = 1000$; (a) Inner liquid with $d_o - 1 = 0{\cdot}25$; (b) Outer liquid with $d_i - 1 = -0{\cdot}2$. Upper graphs, bulging type; lower graphs, sloshing type.

stiffness, and *vice versa*. In the results therefore, the order of the natural frequencies of the sloshing-type and the bulging-type may depend on the values of $\bar{\sigma}_j$. In Figure 7, for example, the natural frequency variation is presented as a function of the tension parameter of the outer liquid $\bar{\sigma}_o$, when $\alpha = 0{\cdot}5$, $d_o - 1 = 0{\cdot}25$, $\beta = 0{\cdot}25$, $m = 1$, $\bar{\rho}_o = 0{\cdot}13$, $\overline{h} = 50$. In this case the surface tension of the inner liquid is fixed at $\bar{\sigma}_i = 1{\cdot}0 \times 10^{-14}$. In the figure, the lowest three natural frequencies of the liquid and elastic structure are presented. The sloshing natural frequencies around a rigid surface are shown as broken lines, for reference. When starting from small values of the surface tension σ_o, increasingly

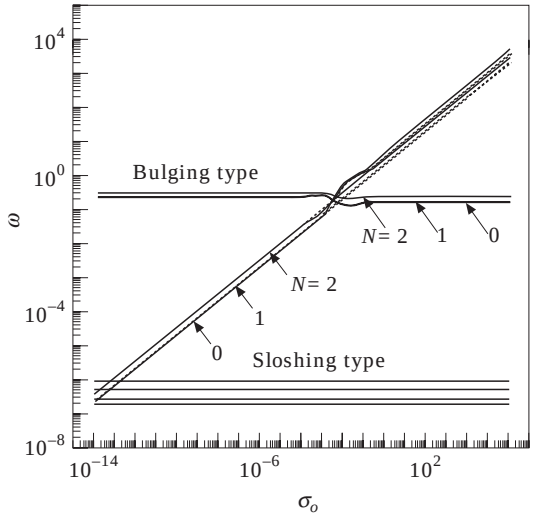

Figure 7. Effect of surface tension parameter of the outer liquid $\bar{\sigma}_o$ on the coupled natural frequency: $\alpha = 0{\cdot}5$, $d_o - 1 = 0{\cdot}25$, $d_i - 1 = -0{\cdot}2$, $\beta = 0{\cdot}25$, $m = 1$, $\bar{\rho}_j = 0{\cdot}13$, $\bar{\sigma}_i = 1{\cdot}0 \times 10^{-14}$, $\overline{h} = 50$.

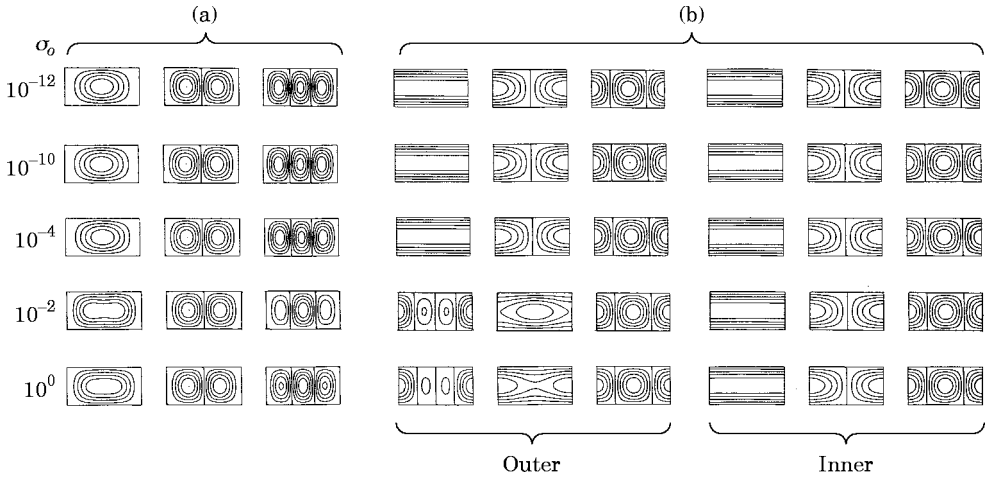

Figure 8. Effect of surface tension parameter of the outer liquid $\bar{\sigma}_o$ on the coupled natural vibration mode: $\alpha = 0{\cdot}5$, $d_o - 1 = 0{\cdot}25$, $d_i - 1 = -0{\cdot}2$, $\beta = 0{\cdot}25$, $m = 1$, $\bar{\rho}_j = 0{\cdot}13$, $\bar{\sigma}_i = 1{\cdot}0 \times 10^{-14}$, $\bar{h} = 50$; (a) Bulging type; (b) Sloshing type.

one finds that after exchanging the order of the natural frequencies of each type, sloshing natural frequencies of the outer liquid become higher than the uncoupled values presented as broken lines, while bulging-type natural frequencies become lower than before. Corresponding mode changes are shown in Figure 8. They are presented as contour lines of the vibration mode. A similar tendency can be seen when changing the surface tension parameter of the inner liquid $\bar{\sigma}_i$ while keeping the value of $\bar{\sigma}_o$.

4.3. UNSTABLE REGION

In the foregoing results, depending on the vibration mode, the thickness of liquid layers, apex angle, α, and aspect ratio, β, some natural vibrations become unstable and frequencies vanish, i.e., see Figures 3 and 4. The unstable regions in which the natural

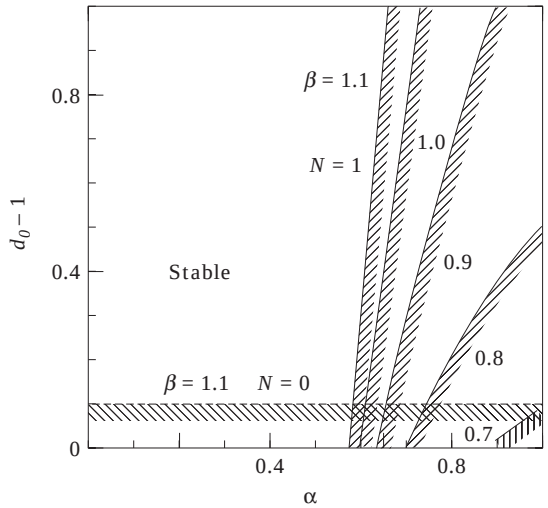

Figure 9. Unstable region of the $N = 0$ and $N = 1$ mode of a liquid *outside* a rigid cylindrical surface: $m = 1$, $\bar{\sigma}_o = 1{\cdot}0 \times 10^{-14}$. Key: — —, $N = 0$; ——, $N = 1$.

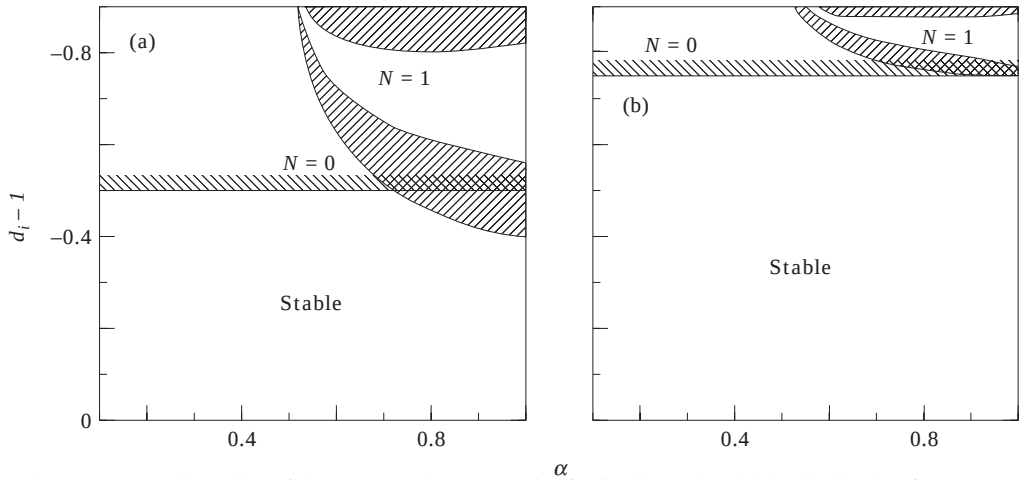

Figure 10. Unstable region of the $N = 0$ and $N = 1$ mode of a liquid *inside* a rigid cylindrical surface: $m = 1$, $\bar{\sigma}_o = 1{\cdot}0 \times 10^{-14}$; (a) $\beta = 0{\cdot}5$; (b) $\beta = 0{\cdot}25$.

frequency vanishes will now be considered. In Figure 9, the unstable regions of the natural frequency of the *outer* liquid layer attached around a rigid cylinder are shown with apex angle α and liquid thickness $d_o - 1$, whilst varying the aspect ratio parameter $\beta = 0{\cdot}7, 0{\cdot}8, 0{\cdot}9, 1{\cdot}0, 1{\cdot}1$. In the figure, solid lines and broken line correspond to the critical boundaries of the mode $N = 1$ and $N = 0$, respectively. Unstable regions are the right side or downward region of the curves.

For the mode with $N = 1$, when β decreases from 1·1 to 0·7, the unstable region narrows down to the region in which the curved wall assumes nearly a circular shell covered by a liquid of smaller layer thickness. The unstable region for the mode $N = 0$ does not exist, if $\beta < 1$, appears at $\beta = 1{\cdot}1$ and does not depend on the apex angle α.

Next, the unstable regions for the liquid attached *inside* the rigid the rigid cylinder will be considered. In Figure 10(a), the unstable regions for an aspect ratio $\beta = 0{\cdot}5$ are shown. The mode $N = 0$ becomes unstable at $d_i - 1 \leqslant -0{\cdot}5$ and is independent of α. The unstable regions for the mode $N = 1$ are given by α, $d_i - 1$, and β. For example one notices two unstable regions for $\alpha = 0{\cdot}8$.

The results when the aspect ratio β decreases to 0·25 are shown in Figure 10(b). Comparing them with $\beta = 0{\cdot}5$ (shown in Figure 10(a)), one notices a shift of the unstable region for the mode $N = 0$ to $d_i - 1 \leqslant -0{\cdot}75$.

From these results, one finds that the unstable boundary for the mode $N = 0$ corresponds to the β value, $\beta = d_j$, $j = i$ and o. The unstable region for the mode $N = 1$ is dependent on α, $d_j - 1$, and β. These unstable regions come from the negative values in the parentheses in equation (23).

5. CONCLUSIONS

A theoretical analysis has been carried out in a zero-gravity condition, on the linear free hydroelastic vibration of liquid layers attached to both inside and outside of a sector cylindrical shell. In the analysis, the liquids are assumed to be frictionless ideal liquids with free surfaces, while the motion of a sector shell is described by the thin elastic shell equations by Flügge. After applying the Galerkin method, the problem yields an eigenvalue problem from which the coupled natural frequencies and vibration modes can be obtained as an eigenvalue and eigenvector, respectively.

In the numerical calculations, the influence of some system parameters, such as apex angle, aspect ratio, thickness ratio, circumferential wave number, liquid thickness, surface tension, density ratio, on the vibration characteristics of a coupled system are investigated. The unstable regions in which the natural frequencies vanish were also clarified.

On the variation of the uncoupled natural frequency of a liquid inside or outside a rigid cylindrical wall with apex angle α, the natural frequency of the mode $N = 1$ with $m = 1$ suddenly changes at $\alpha = 0{\cdot}5$. And when the liquid is attached *outside* the shell, the natural vibration of the mode $N = 1$ with $m = 1$ becomes unstable for large values of α and thinner regions, depending on the aspect ratio β of the sector shell. If the liquid is *inside*, as the aspect ratio β decreases, the unstable boundary shifts to a thicker liquid region in the mode $N = 1$.

The unstable region for the mode $N = 0$ is predicted by β and is independent of α.

With an increase in liquid thickness, the coupled sloshing type natural frequency rapidly increases at the region $0 < d_o - 1 < 0{\cdot}2$ and tends to a gradually increased value when the liquid is attached *outside* the shell, while it rapidly increases at the region $d_i - 1 < -0{\cdot}7$, $N = 2$ when the liquid is *inside* the shell. These can be seen when the liquids are attached both inside and outside the shell.

REFERENCES

1. T. Balenduce, K. K. Aug, P. Paramasivam and S. L. Lee 1982 *International Journal of Mechanical Science* **24**, 47–59. Free vibration analysis of cylindrical liquid storage tanks.
2. M. L. Baron and R. Shalak 1962 *Proceedings of the American Society of Civil Engineering* **88**, 17–43. Free vibrations of fluid-filled cylindrical shells.
3. H. F. Bauer 1970 *Zeitschrift für Flugwissenschaften* **18**, 117–134. Hydroelastische Schwingungen im aufrechten Kreiszylinderbehälter.
4. H. F. Bauer and J. Siekmann 1971 *Ingenieur-Archiv* **40**, 266–280. Dynamic interaction of a liquid with the elastic structure of a circular cylindrical container.
5. H. F. Bauer 1973 *Zeitschrift für Flugwissenschaften* **21**, 202–213. Hydroelastische Schwingungen in einem starren Kreiszylinder bei elastischer Flüssigkeitsoberflächenabdeckung.
6. H. F. Bauer 1986 *International Journal of Solids and Structures* **22**, 1471–1484. Coupled frequencies of a hydroelastic viscous liquid system.
7. H. F. Bauer 1987 *Journal of Sound and Vibration* **113**, 217–232. Coupled frequencies of a hydroelastic system consisting of an elastic shell and frictionless liquid.
8. H. F. Bauer 1987 *Journal of Sound and Vibration* **119**, 249–265. Hydroelastic oscillations of a viscous infinitely long liquid column.
9. P. G. Bhuta and L. R. Koval 1964 *ZAMP* **15**, 466–480. Coupled oscillations of a liquid with a free surface in a tank having a flexible bottom.
10. P. G. Bhuta and L. R. Koval 1964 *Journal of the Acoustical Society of America* **36**, 2071–2079. Hydroelastic solution of the sloshing of a liquid in a cylindrical tank.
11. W.-H. Chu 1963 *Transactions of ASME*, *Journal of Applied Mechanics* (*E*) **30**, 532–536. Breathing vibrations of a partially filled cylindrical tank-liner theory.
12. M. A. Haroun and G. W. Housner 1981 *Transactions of ASME*, *Journal of Applied Mechanics* (*E*) **48**, 411–418. Earthquake response of deformable liquid storage tanks.
13. A. A. Lakis and M. P. Paidoussis 1971 *Journal of Sound and Vibration* **19**, 1–15. Free vibration of cylindrical shells partially filled with liquid.
14. A. W. Leissa 1973 *NASA SP*-288. *Washington*, *D.C*. Vibration of Shells.
15. U. S. Lindholm, D. D. Kana and H. N. Abramson 1962 *Journal of Aerospace Science* **29**, 1052–1059. Breathing vibrations of a circular cylindrical shell with an internal liquid.
16. H. F. Bauer and W. Eidel 1993 *Journal of Fluids and Structures* **7**, 783–802. Hydroelastic vibrations in a circular cylindrical container with a flexible bottom in zero gravity.
17. H. F. Bauer 1992 *Journal of Fluids and Structures* **6**, 603–632. Hydroelastic oscillations of rotating liquid-structure systems in zero gravity.

18. H. F. BAUER and K. KOMATSU 1994 *Journal of Fluids and Structures* **8**, 817–831. Coupled frequencies of a hydroelastic system of an elastic two-dimensional sector-shell and frictionless liquid in a zero gravity.
19. M. CHIBA and H. F. BAUER 1998 *Transactions of ASME*, *Journal of Vibration and Acoustics* **120**, 54–62. Free hydroelastic vibrations of a liquid attached to a cylindrical sector shell in a zero-gravity condition.
20. W. Flügge 1957 *Statik und Dynamik der Schalen*. Berlin: Springer; second edition.